Multi-objective Model-Predictive Control for Dielectric Elastomer Wave Harvesters.

Matthias K. Hoffmann * **Lennart Heib** * **Gianluca Rizzello** **
Giacomo Moretti *** **Kathrin Flaßkamp** *

* *Systems Modelling and Simulation,*
(e-mail: {matthias.hoffmann, kathrin.flasskamp}@uni-saarland.de,
lennartheib@gmail.com)
** *Adaptive Polymer Systems,*
(e-mail: gianluca.rizzello@imsl.uni-saarland.de)
*** *Università degli Studi di Trento, (e-mail: giacomo.moretti@unitn.it)*
* *and* ** *from Saarland University, Saarbrücken, Germany.*

Abstract:

Keywords: Multi-objective Optimal Control, Model-predictive Control, Energy Harvesting, Non-Linear Optimization, Dielectric Elastomer Generators

1. INTRODUCTION

2. MODEL AND PROBLEM STATEMENT

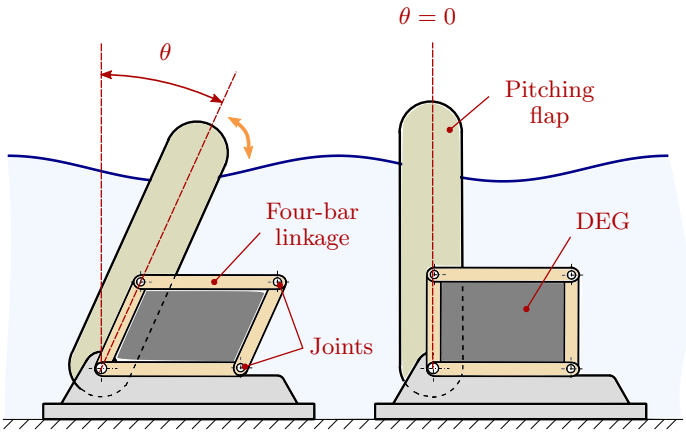

Fig. 1. Wave surge converter: A flap mounted to the sea floor is tilted by the wave motion. It is displayed in a generic (left) and the vertical equilibrium position (right).

2.1 Background

Model-predictive Control (MPC) arose from optimal control as one answer on how to "close the loop" (Rawlings et al. (2017)). In optimal control, a system's behaviour is predicted for a time called the prediction horizon t_f into the future, while optimising the inputs to the system, such that a cost function is minimised. The working principle of MPC is repeatedly measuring the system's state, solving an Optimal Control Problem (OCP), and applying the first few of the calculated inputs.

Notation: The subindex MPC marks applied inputs and resulting states of the actual system.

2.2 System

In this work, we investigate the MPC of the wave surge converter (see, e.g. Whittaker and Folley (2012)), displayed in Fig. 1. The device is pivoted to the sea, such that incoming waves excite an oscillatory motion. This distorts a dielectric elastomer generator (DEG) mounted to a deformable parallelogram, Moretti et al. (2014). Through this parallelogram, the DEG applies a torque to the flap towards the equilibrium position $\theta = 0$. Applying a voltage to the DEG adds an electrostatically-induced torque in the same angular direction, making the system stiffer.

When a voltage is applied to the DEG, charge carriers accumulate in the DEG. By deforming the parallelogram to a smaller area (increased θ), the charge density increases, such that energy can be extracted. As we showed in our previous work Hoffmann et al. (2022), controlling the input to maximise the energy extracted from the system requires application of large voltages, damaging the DEG-material over time, and resulting in system failure after too much damage accumulated Chen et al. (2019). For that reason, we also took the damage into consideration as a second control goal, resulting in lower electric fields in the DEG.

2.3 Model

The dynamics of the wave surge

$$\begin{aligned}\begin{bmatrix}\dot\theta\\ \dot\delta\\ \dot z\end{bmatrix} &= \begin{bmatrix}0 & 1 & 0^{1\times n}\\ -I_\mathrm{h}^{-1}K_\mathrm{h} & -I_\mathrm{h}^{-1}B_\mathrm{h} & -I_\mathrm{h}^{-1}C_\mathrm{r}\\ 0^{n\times 1} & B_\mathrm{r} & A_\mathrm{r}\end{bmatrix}\begin{bmatrix}\theta\\ \delta\\ z\end{bmatrix} +\\ &\quad + \begin{bmatrix}0\\ I_\mathrm{h}^{-1}\\ 0^{n\times 1}\end{bmatrix}(d - C_0\theta u)\\ \theta(0) &= \theta_0,\ \delta(0) = \delta_0,\ z(0) = z_0,\end{aligned} \tag{1}$$

contain the equation of angular motion and the wave loads generated by the interaction of the waves with the flap. Here, $\delta = \dot\theta$ describes the flap's angular velocity, $z \in \mathbb{R}^n$

the n-dimensional state vector for wave radiation (Yu and Falnes (1995)) and d, the force the waves exert on the flap. The input u is the electrostatic force generated by the DEG when a voltage v is applied. Since the DEG's electrostatic force is proportional to the v^2, u is restricted to be positive. add u constraint explanation?

$$u \leq (E_{\mathrm{bd}} h_{\mathrm{l}})^2 / \cos^2(\theta), \tag{2}$$

2.4 Cost functions

Our aim is the simultaneous minimisation of damage and maximisation of extracted energy, which we will employ in a multi-objective Optimal Control (MOOCP) setting. The extracted energy cost function is modelled as the negative generated energy

$$\begin{aligned} J_1 &= \Psi(t_{\mathrm{f}}) - \Psi(0) + \int_0^{t_{\mathrm{f}}} \left(B_{\mathrm{h}} \delta^2 + z^\intercal S_{\mathrm{r}} z + \frac{u}{R_0} - d\delta \right) \mathrm{d}t \\ \text{with } \Psi &= \frac{1}{2} I_{\mathrm{h}} \delta^2 + \frac{1}{2} K_{\mathrm{h}} \theta^2 + \frac{1}{2} z^\intercal Q_{\mathrm{r}} z + \frac{1}{2} C_0 \left(1 - \theta^2\right) u, \end{aligned} \tag{3}$$

with the storage function Ψ including kinematic, potential, electrostatic, and hydrodynamic energy contributions. Dissipations due to viscous, hydrodynamic, and electrical losses, and the power input by the incident wave are considered via the integral terms.

Under the assumption, that damage only starts accumulating after the applied electric field exceeds a threshold E_{th}, the cost function can be formulated as

$$J_2 = \alpha \int_0^{t_{\mathrm{f}}} \left(\max\{\cos^2(\theta) u - E_{\mathrm{th}}^2 {h_{\mathrm{l}}}^2, 0\} \right)^{n_{\mathrm{d}}} \mathrm{d}t, \tag{4}$$

with a normalisation factor α rendering J_2 dimensionless, and an experimental parameter n_{d}. too close to Mathmod paper?

Equations (1), (2), (3), and (4) formulate the MOOCP

Problem 1.

$$\begin{aligned} &\underset{u(t)}{\text{minimize}} \quad (J_1, J_2) \\ &\text{subject to dynamics (1)} \\ &\qquad 0 \leq \cos^2(\theta) u \leq (E_{\mathrm{bd}} h_{\mathrm{l}})^2. \end{aligned} \tag{5}$$

that is solved inside the MPC.

3. METHODS

3.1 Discretisation and simplification of the OCP

In order to solve the Problem 1, we employ direct methods for optimal control to first formulate the OCP as a non-linear program (NLP) (see Gerdts (2011)). Using gradient-based methods, the discretised optimal control sequence is calculated. The integral terms inside the cost functions have to be approximated. We do so by adding the integrand to the dynamics

$$\begin{aligned} \dot{\Upsilon}_1 &= B_h \delta^2 + z^\intercal S_r z + \frac{u}{R_0} - d\delta \\ \dot{\Upsilon}_2 &= \left(\max\{u - E_{th}^2 h_l^2, 0\} \right)^{n_d}, \end{aligned}$$

with

$$\Upsilon_1(0) = \Upsilon_2(0) = 0.$$

Remark, that the term $\cos^2(\theta)$ is simplified to 1, the same is done in the constraint on u. The extended state reads $\xi = [\theta\ \vartheta\ z^\intercal\ \Upsilon_1\ \Upsilon_2]^\intercal$, with the initial value $\xi_0 = [\theta_0\ \vartheta_0\ {z_0}^\intercal\ 0\ 0]^\intercal$

In the following, the discretised values corresponding to their continuous counterparts are marked by square brackets, e.g. the state vector $\xi[k]$, the extended state k time steps into the future. The current state of the system is advanced by one step into the future using the classical Runge-Kutta-Method of 4-th order (RK4), denoted by $F_{RK4}(\xi[k], u[k], u[k+1], d[k], d[k+1])$. Consecutive values for the input and wave excitation are used to model first-order hold (FOH) behaviour. The dynamics can then be expressed with the equality constraints

$$\begin{aligned} \xi[k+1] = F_{RK4}(\xi[k], u[k], u[k+1], d[k], d[k+1]) \\ \forall k \in [0, N-2]] \\ \xi[0] = \xi_0, \end{aligned}$$

where N is the number of time steps t_f is separated into. The cost functions are then $J_1 \approx \Upsilon_1[N-1]$ and $J_2 \approx \Upsilon_2[N-1]$, so that the MOOCP is

Problem 2.

$$\begin{aligned} &\underset{u[1],\ldots,u[N]}{\text{minimize}} \ w_1 J_1 + w_2 J_2 \\ &\text{subject to } \xi[k+1] = F_{RK4}(\xi[k], u[k], u[k+1], \ldots \\ &\qquad d[k]), d[k+1]) \forall\ k \in [0, N-2], \\ &\qquad 0 \leq u[k] \leq (E_{bd} h_l)^2,\ \forall\ k \in [0, N-1] \qquad (6) \\ &\qquad \xi[0] = \xi_0 \qquad (7) \\ &\qquad u[0] = u_0, \qquad (8) \end{aligned}$$

where u_0 is a fixed initial value of 0 for the very first and $u_{\mathrm{MPC}}[k-1]$ for the k-th MPC-step. understandable? The values for Ψ are dropped. Since $\Psi(0)$ is a constant for the FOH formulation, it does not change the optimization problem. Regarding $\Psi(t_{\mathrm{f}})$, $I_{\mathrm{h}}, K_{\mathrm{h}}$ are multiple magnitudes larger than C_0, so their terms dominate the expression of Ψ. The quadratic cost terms push the solution to the equilibrium position $\theta = 0$ at the end of the prediction horizon, an effect unwanted in continuous operation.

3.2 Wave generation

3.3 Adaptive weight selection

When applying MPC, we do not know exactly how the system will perform over the deployment of the control. In the case of the WEC-DEG when driving the system with a fixed weighting, different sea states will result in a different damage accumulation over time. Since the DEG has to be replaced once it breaks down, an operator of multiple DEGs might be interested replacing all of the devices at the same time to save monetary costs. This means, that the breakdown of all the devices has to be synced, e.g. by changing the weighting of the damage cost function in a way, such that the accumulated damage cost at the designated break-down time t_{bd} does not exceed a fixed value J^{d}.

Assume a fixed set w of n_{w} weight combinations sorted from low to high priority for the handled cost function (in our case J_2) and an initial weight index $i_{\mathrm{w}} \in [1, n_{\mathrm{w}}]$. One easy way of deciding, if the damage goal is achievable

with the current weighting is by evaluating the MPC performance over N_p time steps into the past. The average rate of damage accumulation J_{ps} is estimated and the damage at the break-down time is predicted as an average trend. If the predicted damage exceeds J^{d}, i_{w} is decreased by 1. Otherwise, if the predicted damage falls below $c_{\mathrm{d}} J^{\mathrm{d}}$ with $c_{\mathrm{d}} \in [0, 1]$, i_{w} is increased by 1. This is done every N_p steps if the DEG was actuated during that time. Of course, this algorithm just evaluates the performance in hindsight, not using the full potential of MPC. Still, we show that even this very simple heuristic can perform quite well, motivating more elaborate adaptation algorithms.

For an exemplary implementation in MATLAB using the mentioned system, refer to link.

4. NUMERICAL RESULTS

The following simulations were done using MATLAB. The optimisation problems were formulated and solved using the CasADi package by Andersson et al. (2019) and the IPOPT solver by Wächter and Biegler (2006). The panchromatic waves were generated using 50 frequencies with a base frequency of 0.1 Hz, while perfect prediction is assumed.

4.1 Accuracy of model-predictive control

When employing MPC, we cannot expect to get the same results as an OCP with longer prediction horizon would give. By shifting the prediction horizon each time step, new information is provided, potentially leading to largely different input sequences compared to previous solutions. Fig. 2 shows the mean absolute error (MAE) between the ground truth OCP solution over a prediction horizon of 320 s and u_{MPC}. u_{MPC} was calculated using different horizon lengths from 10 to 77 s. As expected, the error decreases for longer prediction horizons. Moreover, it shows that for prediction horizons of length close to the period of the base wave, the error stagnates, indicating that prediction horizons longer than that are recommended. In the following, we will use a 60 s horizon for a good performance while not increasing the OCP's complexity too much.

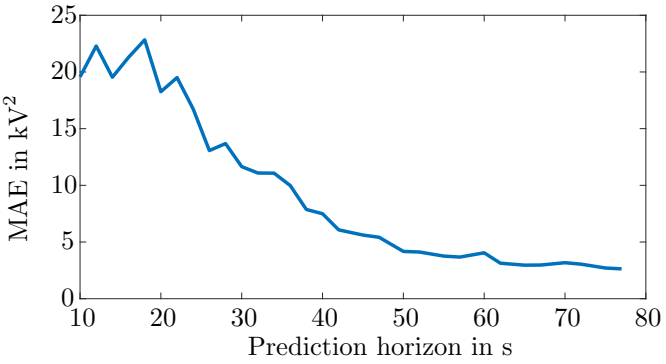

Fig. 2. Mean absolute deviation of u_{MPC} over 320 s from ground truth for different prediction horizon lengths. Ground truth is an OCP over the full horizon.

4.2 Weight selection algorithm

In this section, we evaluate the performance of the simple heuristic weight selection algorithm by simulating the system's behaviour for different sea states. The $n_{\mathrm{w}} = 15$ predetermined weights are evenly distributed between 0.05 and 0.95 with $w_1 + w_2 = 1$. As shown in Fig. 3, this does not result in an even distribution of Pareto points along the Pareto front, but as we will show, even this very simple approach yields nice results.

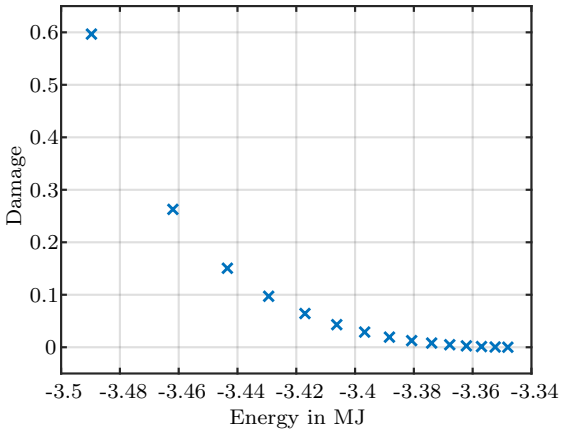

Fig. 3. For an even distribution of weights, the Pareto points are typically not evenly distributed along the Pareto front.

Alternatively, the weights could be found using the adaptive weight determination scheme by Ryu and Min (2019). We compare for three different wave scenarios the performance of the MPC with weight controller for two target damage values $J^{\mathrm{d}} = \{0.3, 0.5\}$. The performance of a weighting is evaluated every 25 s. An increase of the damage weighting is allowed after each evaluation, a decrease only every two evaluations.

Fig. 4 shows the performance of this heuristic weight control for the three different wave excitations by displaying the accumulated damage in the top and the selected index in the bottom plots. Large increase of damage typically happens when, after a long time of weak waves, the sea state changes and stronger waves arrive, showing the need for online adaptations to the controller. In the left example, the waves are all very similar and since the initial weighting would not exploit all the damage, the damage weight is steadily decreased until, for the 0.5 threshold, the index stays around 12. For the second case,

5. CONCLUSION

REFERENCES

Andersson, J.A., Gillis, J., Horn, G., Rawlings, J.B., and Diehl, M. (2019). Casadi: a software framework for nonlinear optimization and optimal control. *Mathematical Programming Computation*, 11(1), 1–36. doi: 10.1007/s12532-018-0139-4.

Chen, Y., Agostini, L., Moretti, G., Berselli, G., Fontana, M., and Vertechy, R. (2019). Fatigue life performances of silicone elastomer membranes for dielectric elastomer transducers: preliminary results. In *Electroactive Polymer Actuators and Devices (EAPAD) XXI*, volume 10966, 1096616. International Society for Optics and Photonics.

Gerdts, M. (2011). *Optimal Control of ODEs and DAEs*. Walter de Gruyter.

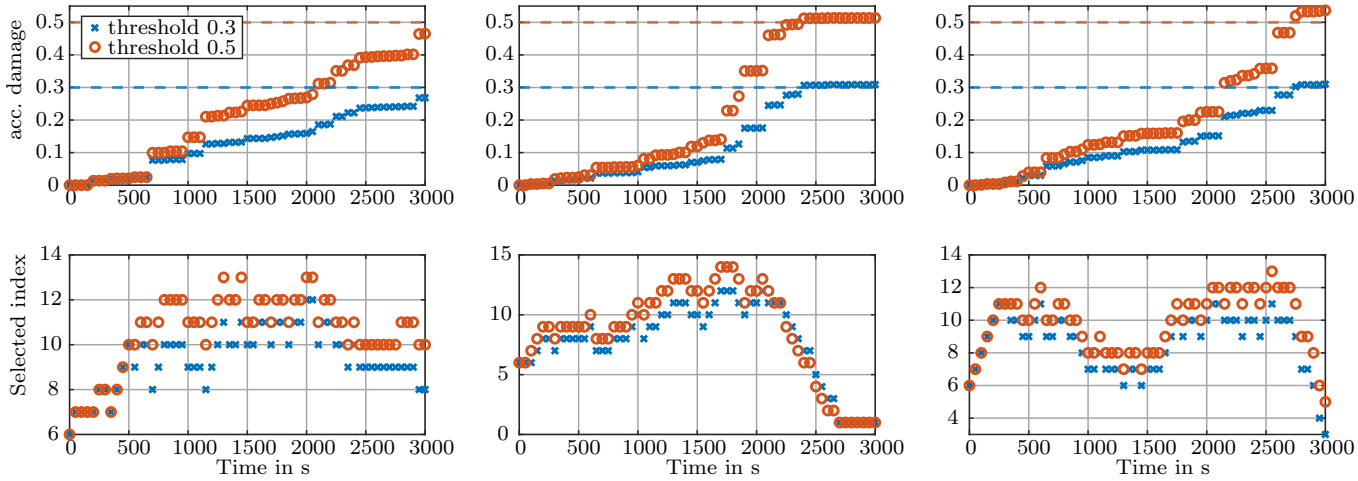

Fig. 4. Evaluation of the MPC with weight controller for three wave scenarios and two target damage values. Every 100th
Top: Accumulated damage over time. Bottom: The selected weight index i_w over time. A lower index corresponds to a higher weighting for the damage cost.

Hoffmann, M.K., Moretti, G., Rizzello, G., and Flaßkamp, K. (2022). Multi-objective optimal control for energy extraction and lifetime maximisation in dielectric elastomer wave energy converters. *IFAC-PapersOnLine*, 55(20), 546–551.

Moretti, G., Forehand, D., Vertechy, R., Fontana, M., and Ingram, D. (2014). Modeling of an oscillating wave surge converter with dielectric elastomer power take-off. In *International Conference on Offshore Mechanics and Arctic Engineering*, volume 45530, V09AT09A034. American Society of Mechanical Engineers.

Rawlings, J.B., Mayne, D.Q., and Diehl, M. (2017). *Model predictive control: theory, computation, and design*, volume 2. Nob Hill Publishing Madison, WI.

Ryu, N. and Min, S. (2019). Multiobjective optimization with an adaptive weight determination scheme using the concept of hyperplane. *International Journal for Numerical Methods in Engineering*, 118(6), 303–319.

Wächter, A. and Biegler, L.T. (2006). On the implementation of an interior-point filter line-search algorithm for large-scale nonlinear programming. *Mathematical programming*, 106(1), 25–57.

Whittaker, T. and Folley, M. (2012). Nearshore oscillating wave surge converters and the development of oyster. *Philosophical Transactions of the Royal Society A: Mathematical, Physical and Engineering Sciences*, 370(1959), 345–364.

Yu, Z. and Falnes, J. (1995). State-space modelling of a vertical cylinder in heave. *Applied Ocean Research*, 17(5), 265–275.